Interactive Rigid-Body Dynamics and Deformable Surface Simulations with Co-Located Maglev Haptic and 3D Graphic Display

Peter Berkelman
Department of Mechanical Engineering
University of Hawaii at Manoa
Honolulu Hawaii, USA
Email: peterb@hawaii.edu

Sebastian Bozlee
Mathematics Department
University of Portland
Portland Oregon, USA
Email: sebbyj@gmail.com

Muneaki Miyasaka
Department of Mechanical Engineering
University of Washington
Seattle Washington, USA
Email: muneaki@uw.edu

***Abstract*—We have developed a system which can combine realtime dynamic simulations, 3D display, and magnetic levitation to provide high-fidelity co-located haptic and graphic interaction. Haptic interaction is generated by a planar horizontal array of cylindrical coils which act in combination to produce arbitrary forces and torques in any direction on magnets fixed to an instrument handle held by the user, according to the position and orientation sensed by a motion tracking sensor and the dynamics of a realtime physical simulation. Co-located graphics are provided by a thin flat screen placed directly above the coil array so that the 3D display of virtual objects shares the same volume as the motion range of the handheld instrument. Shuttered glasses and a head tracking system are used to preserve the alignment of the displayed environment and the interaction handle according to the user's head position. Basic interactive environments have been developed to demonstrate the system feasibility and operation, including rigid bodies with solid contacts, suspended mass-spring-damper assemblies, and deformable surfaces. Interactive physical simulation of these environments requires real-time collision detection between geometric models; numerical, discrete-time numerical integration to calculate the physics of networks of mass, spring, and damper elements; and calculation and actuation of interactive forces to the user in haptic rendering. Incorporating these functions into a single executable requires multiple program threads with various update rates, ideally performed using a multicore processor PC. Details and discussion of various simulations are given with experimental results.**

Keywords- haptics, interaction, simulation

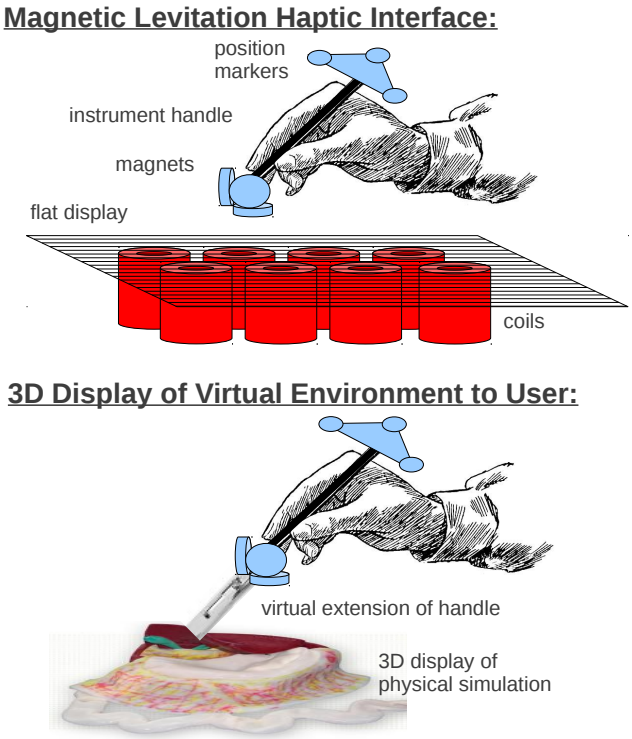

Figure 1: Co-located maglev haptic and 3D graphic display

I. Introduction

The ideal of virtual reality and haptic interfaces is to physically interact with simulated objects with the highest possible fidelity in both the graphical display and the kinesthetic forces and torques sensed by the user during interaction. Computer-generated graphics can produce highly realistic, dynamic 3D imagery in real time, but haptic interfaces are generally based on single point contact feedback, tactile cues, and linkage devices which have various limitations in their force and motion ranges, frequency response bandwidth, and resolution.

Our system combines a graphical display with a large range of motion magnetic levitation device, as shown in Fig. 1. The graphical display is placed directly above a horizontal array of cylindrical coils and underneath the instrument handle held by the user, so that electromagnetic forces and torques can be generated on magnets embedded in the handle as the instrument is moved by the user into contact with the displayed simulated environment.

The magnets embedded in the instrument handle, the coil array with its current amplifiers, and the motion tracking sensor with its infrared LED markers, function together as a magnetic levitation system. Several variations of magnet configurations have been developed for stable levitation with the planar coil array, each providing a different combination

2013, © Copyright by authors, Published under agreement with IARIA - www.iaria.org

of parameters such as mass and size; force, torque and impedance ranges; and vertical translation and tilt (roll and pitch) rotation ranges. For the interactive simulations described here, two-magnet and four-magnet configurations were used, where the two-magnet handle provides greater feedback force and torque capabilities and the four-magnet handle is less massive, smaller, and provides somewhat greater vertical and rotational motion ranges. Both magnet configurations provide motion ranges of at least 100x100 mm horizontally, approximately 50 mm vertically, with unlimited yaw and tilt up to at least 35 degrees.

A secondary, slower and less precise motion tracking system tracks the position of the user's head so that the 3D views are generated correctly according to the position of each of the user's eyes. A pair of shuttered glasses, synchronized to the update rate of the graphics on the monitor, is worn by the user so that each eye sees a different image as the shutters alternate. In practice, this head tracking system allows the user to observe the handheld instrument and the 3D displayed environment together from the side and from above, in a natural ergonomic position for hand-eye coordination during dextrous manipulation of a handheld instrument or tool. Examples of relevant dextrous tool manipulation tasks include any writing, carving, or cutting tasks, operation of wrenches or screwdrivers, and medical needle manipulation for suturing, injections, and biopsy.

The real-time haptic interaction and graphical display are generated from a dynamic simulation which must perform collision detection, finite element deformation, and haptic rendering sufficiently quickly to support graphical updates at 30-60 Hz and haptic interaction and magnetic levitation at 800-1000 Hz. These tasks are sufficiently computationally intensive to be the limiting factor regarding the resolution and realism of the simulated environment.

This paper is an extended version of the previously published conference paper [1]. A survey of similar research in co-located haptics and graphics, magnetic levitation, and interactive physical simulation areas is given in Section II. The implementation details are given in Section III for the magnetic levitation subsystem and Section IV for the co-located 3D display subsystem. The physical simulation software and haptic rendering details are given in Section V. Force and motion experimental results for selected interactive simulations are given in Section VI. Continuing work is described in Section VII followed by a conclusion section.

II. Related Work

The realization of our interactive system depends on the performance and integration of technology in the areas of maglev haptics, graphics, and physical simulation. Relevant prior work in each of these areas is surveyed below.

A. Co-Located Haptics and Graphics

3D graphics and haptic force and/or torque feedback can be generated at the same location by simply placing the 3D display behind the haptic interaction device, however, this method has two drawbacks. First, the body of the haptic interface device partially occludes the display, and second, there may be a significant difference produced between the perceived location of the displayed imagery and the surface of the screen, so that the convergence and focal distance of the user's eyes do not match, which is unnatural and may cause discomfort to the user.

ReachIn, *ImmersiveTouch*, and *SenseGraphics* systems [2] use a partially silvered mirror between the head and hand of the user, so that the display can be moved out of the way and the focal and convergence distances of the user's eyes can be matched. The haptic device and the user's hand do not occlude the 3D graphics behind them, but rather the real and virtual environments are superimposed and semitransparent due to the half-silvered mirror, which may be a distraction to the user.

The "what you see is what you feel" system [3] uses a thin flat display with a camera behind it. The video image of the user's hand is then extracted from the camera view using a green screen chroma-key technique, and rendered in the virtual environment. Holographic display [4] using a diffraction grid reflector and multiple projectors is another method which has been used for haptic and graphic co-location.

Other systems which have combined co-located haptics and graphics for user interaction have included mechanisms built into the display monitor [5], a cable-driven pen above the monitor [6], or linear induction motors with graphics projected from overhead [7]. The haptic feedback provided by these systems is limited, however, to only planar forces and torques, or predetermined locations, whereas the haptic interaction in our system provides full six degree-of-freedom rigid-body force and torque feedback over large ranges of translation and rotation.

Comparative studies have shown [8] [9] evidence of improved perception and performance from co-located haptic interaction.

B. Haptic Magnetic Levitation

Hollis and Salcudean first developed Lorentz force magnetic levitation devices [10] and applied them to haptic interaction and force-feedback teleoperation. Lorentz force magnetic levitation haptic interaction development continued with other more specialized device designs [11] [12] and larger range devices developed by Berkelman [13] [14].

Lorentz magnetic levitation is based on the Lorentz force F, which is directly proportional to both electric current I and magnetic field flux density B, integrated along the current path l, expressed as $F = \int B \times I \, dl$. Fixed magnet assemblies and a set of six coil windings on the levitated platform must be arranged so that forces and torques can

2013, © Copyright by authors, Published under agreement with IARIA - www.iaria.org

be produced in any direction as required for stable 6 DOF position feedback motion control and stable levitation. The advantage of the Lorentz actuation method compared to electromagnetic attraction and repulsion forces is that the force to current and flux density relationships are linear, and there is no direct dependence on position, so that the coil current to force and torque vector transformation is nearly constant over the motion range of the levitated body.

The range of motion in translation for Lorentz levitation is limited by the size of the gaps between the magnet faces in which the magnetic fields are concentrated, and the range in rotation is limited by the active areas of each coil in which the coil windings pass through the magnetic fields. To maximize the range of motion in both translation and rotation, it is best to arrange large-area flat-wound coils onto a thin hemispherical shell, with a user interaction handle mounted at its center.

Compared to linkage-based haptic devices such as the Sensable Phantom [15], the Novint Falcon [16], and the Force Dimension Delta [17], Lorentz levitation haptic interface devices can provide much greater forces and torques greater than 10 N and 1.0 N-m, and control stiffnesses of 10 N/mm are achievable without difficulty. Closed-loop position control bandwidths are greater than 100 Hz in all directions in both translation and orientation. Lorentz levitation motion ranges are much more limited, however, as the Carnegie Mellon and Butterfly Haptics devices have ranges of approximately 25 mm and 30 degrees of rotation, and a University of Hawaii prototype with a modified magnet and coil configuration has a range of 50 mm and 60 degrees of rotation [18]. Overheating of the actuation coils is not a problem, as the levitated hemispherical shell is quite thin with a large surface area and acts as an effective heat dissipator.

The general design and function of the planar coil array magnetic levitation system used here is described in [19]. This system uses a fixed planar array of cylindrical coils to levitate a platform of one or more cylindrical magnets. The yaw of the levitated platform is unlimited and its horizontal motion range is determined by the size of the planar array. Vertical levitation distances of up to 75 mm and tilt angles of 45 degrees are achievable, depending on the mass of the levitated platform and the dimensions of the magnets used.

Similar tabletop-scale large range magnetic levitation systems have been developed for suspension of models in wind tunnels [20] and for micromanipulation using pole pieces to shape magnetic fields [21].

C. Realtime Physical Simulation Libraries and Haptic Rendering Programming Interfaces

Realistic software simulations of dynamic physical environments have been developed by Baraff both for rigid [22] and deformable [23] objects, including efficient collision and reaction force detection and surface friction. Freely available physical simulation software packages include the SOFA framework [24] [25], Bullet Physics, and the PhysX library from NVIDIA. Higher resolution and performance can be obtained by using precomputed deformation modes [26] and 6-DOF haptic rendering including torque feedback as well as force on an interactive instrument can be integrated with simulations [27].

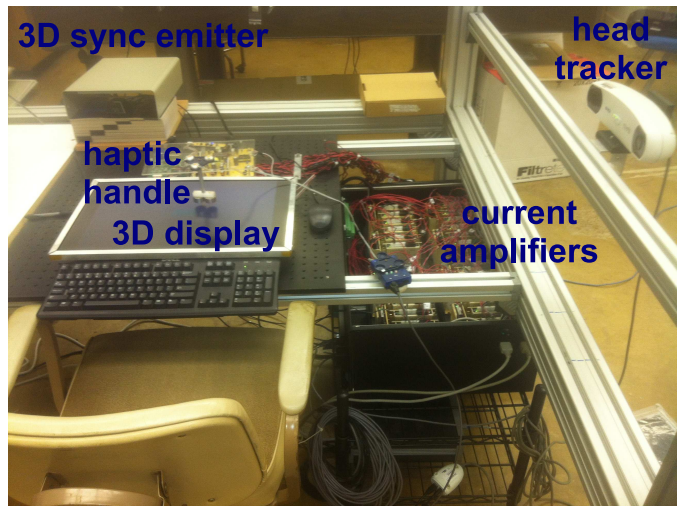

Figure 2: Implemented system

Realistic haptic interaction with dynamic simulated environments typically requires realtime computation at update rates in the range of 1000 Hz. Collision detection, calculation of rigid body contacts [28], and simulation of physical dynamics, must be performed concurrently with the control of the haptic interaction device. Virtual coupling, using a virtual spring and damper to connect an interaction object in the simulated environment with the physical object grasped by the user [29], is a straightforward method to integrate a simulated environment with a haptic interaction device.

Several software packages are freely available for haptic rendering and realtime physical simulation. H3D [30] and Chai3D [31] include driver interfaces for common commercial haptic interface devices such as the Sensable Technologies Phantom [15]. A programming interface is also available with the magnetic levitation haptic interface from Butterfly Haptics LLC [32].

III. Implemented Magnetic Levitation System

The motion tracking, magnetic levitation control, haptic rendering, physical simulation, and graphical display in our current system are all executed in real time in separate threads on a single quad-core PC in Linux 2.6. GNU C/C++ was used for all programming. An initial demonstration concept of the system with a simulation of a single paddle instrument and a ball rolling on a plane, an earlier magnet and coil configuration, and a conventional 2D display was demonstrated previously [33]. The current system is shown

2013, © Copyright by authors, Published under agreement with IARIA - www.iaria.org

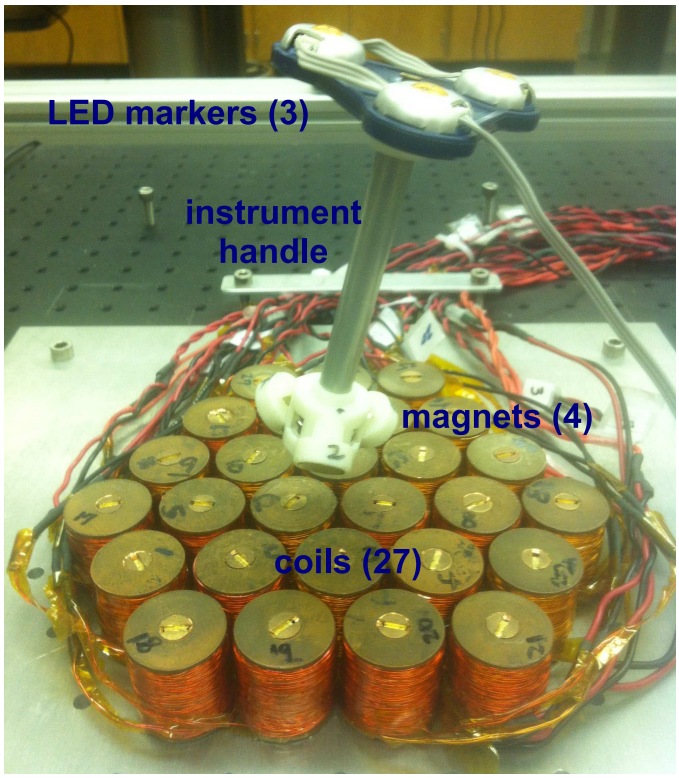

Figure 3: Levitated 4-magnet instrument

in Fig. 2, including the planar 3D display, haptic instrument handle, current amplifiers, and head tracker.

A. Magnetic Levitation Hardware Setup

The motion tracking of the handheld instrument in our system is done using a Northern Digital Optotrak Certus position sensor and three infrared Smart Markers. Motion tracking updates are provided at 860 Hz with a position resolution of approximately 0.01 mm for each marker. Actuation forces and torques are generated by a closely packed array of 27 cylindrical coils, each with 1000 windings, 25 mm diameter, and 30 mm height. Either a two-magnet or four-magnet instrument handle can be used with the system; the two-magnet 125 g instrument can provide greater haptic forces and torques but is more massive and bulky, and the smaller 75 g four-magnet instrument occludes the user's view of the display less due to its compact size. Forces are limited to approximately 4 N due to heating of the actuation coils, although higher momentary peak forces are possible.

The four-magnet instrument is shown in Fig. 3, levitated above the 27-coil array at a height of 30 mm and a tilt angle of 20 degrees. This coil array is underneath the 3D display monitor shown in Fig. 2. The motion tracker for the haptic instrument is mounted on a rigid frame at ceiling level, looking downwards.

B. Design and Control Software

The general design and evaluation methods used in the development of the magnetic levitation system are described in detail in [34]. Electromagnetic modeling of the forces and torques between each magnet and coil was performed using Mathematica [35] from Wolfram Research and Radia [36], a freely available software package developed by the European Synchrotron Radiation Facility.

At each sensor update of the levitation control system, the coil current to levitation force and torque transformation matrix is calculated according to the levitated body position and orientation and the precomputed electromagnetic models, control forces and torques are generated according to proportional and derivative (PD) error gain control laws for each of the total 6 degrees of freedom in translation and rotation, and updated coil currents are calculated using the pseudoinverse of the coil current to force and torque transformation matrix.

IV. Co-Located 3D Graphical Display

The NVIDIA 3D Vision package was used with Linux drivers to provide 3D display of the simulated environment. This package uses shutter glasses which are synchronized with the graphics card by an infrared emitter box. A Quadro 4000 graphics card was used with a ViewSonic vm2268 monitor with a 120 Hz update rate. OpenGL and GLUT graphics libraries are used for the 3D graphics rendering.

The case of the monitor was removed and backplane circuit boards and wiring were moved so that the monitor backlight and display could be placed directly on the coil array. The combined thickness is under 10 mm, so that haptic forces and torques can be applied to the handheld instrument up to a vertical height of at least 60 mm. Magnetic fields from the instrument magnets and coil array were not found to interfere with the display, and there are no ferromagnetic components in the display to interfere with the magnetic levitation system. A thin sheet of polycarbonate plastic was fixed on top of the monitor screen for protection from impacts from the magnets and instrument, and an aluminum frame was built to protect the edges of the display.

Head tracking was implemented using a Northern Digital Polaris Vicra and passive reflective markers to produce correct 3D display according to the position of each eye. The spatial position and orientation of the shutter glasses from the positions of four reflective markers fixed to the glasses. Position and orientation data were updated at a 10 Hz rate with a resolution of approximately 0.1 mm for each marker. It would be possible to track both the magnet instrument and and the user's head using a single motion tracking system, but this would require using wired infrared markers on the 3D shutter glasses, slowing down the update rate of the magnetic levitation localization due to the additional LED markers on the glasses, and mounting the localizer at least

2013, © Copyright by authors, Published under agreement with IARIA - www.iaria.org

Figure 4: Shutter glasses with synchronization signal transmitter, reflective markers, and localizer for 3D graphic display with head tracking

3.5 m high so that its sensing volume includes the location of the glasses.

As both the Optotrak and Polaris motion trackers use infrared position sensing, and 3D Vision systems uses infrared communication to synchronize display frames with the shutter glasses, it is necessary to ensure that each infrared system does not interfere with the others. In our system, each set of emitters and receivers are oriented in orthogonal directions and positioned so that each emitter is only visible to its corresponding receiver. The Optotrak sensor is mounted above the table looking down at the LEDs on the instrument, the Polaris is mounted on the side of the table to track the reflective markers on the side of the glasses, and the synchronization emitter is mounted at the front of the tabletop. The synchronization emitter, shutter glasses with reflective position markers, and head tracking localizer are shown in Fig. 4.

The 3D vision system as described produced reasonably convincing 3D graphics but had a number of minor shortcomings. The horizontal position of the monitor resulted in a reduction in brightness observed by the user due to the change in viewing angle. Light reflections from the glossy screen could be distracting, but the room can be darkened to eliminate this problem. The 10-15 Hz update rate of the head tracking system and its communication latency produce a noticeable lag if the user's head moves quickly. The motion tracking reflectors on the side of the shutter glasses are also somewhat cumbersome. Many of the shortcomings of the present head tracking system could be overcome by using a radio-frequency emitter, currently available from NVIDIA, rather than an infrared signal for the shutter glasses synchronization, and using an optical tracker with a quicker update rate.

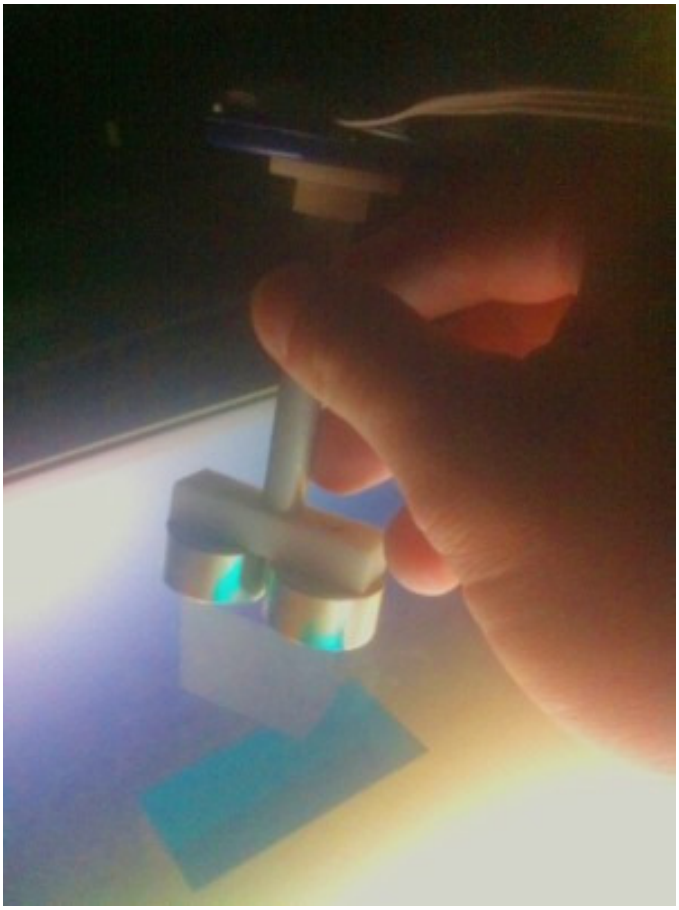

Figure 5: Peg in hole simulation with grapsed tool aligned with graphical peg

V. Haptic Simulations

Basic interactive simulations which have been implemented on our system at present include point, edge, and face contacts between simple solid shapes such as square peg-in-hole insertion as shown in Fig. 5, simple dynamic environments including suspended masses and springs, and rolling objects. These simple initial simulations allow the dynamics and contact models of the environments to be modified and adjusted to provide the most realistic haptic interaction while preventing unstable dynamics.

A more sophisticated simulation which involves an instrument contacting a deformable surface is shown in Fig. 6. In this simulation, a virtual extension is added to the actual haptic instrument handle, and the deformation of the surface and reaction forces and torques on the instrument are calculated at the haptic update rate. Damping is added to the internal dynamics of the deformable body and the surface dynamics during contact with the haptic instrument.

The MLHI library and programming interface, originally from Butterfly Haptics LLC, has been adapted for use with our system and can be used for haptic rendering and

2013, © Copyright by authors, Published under agreement with IARIA - www.iaria.org

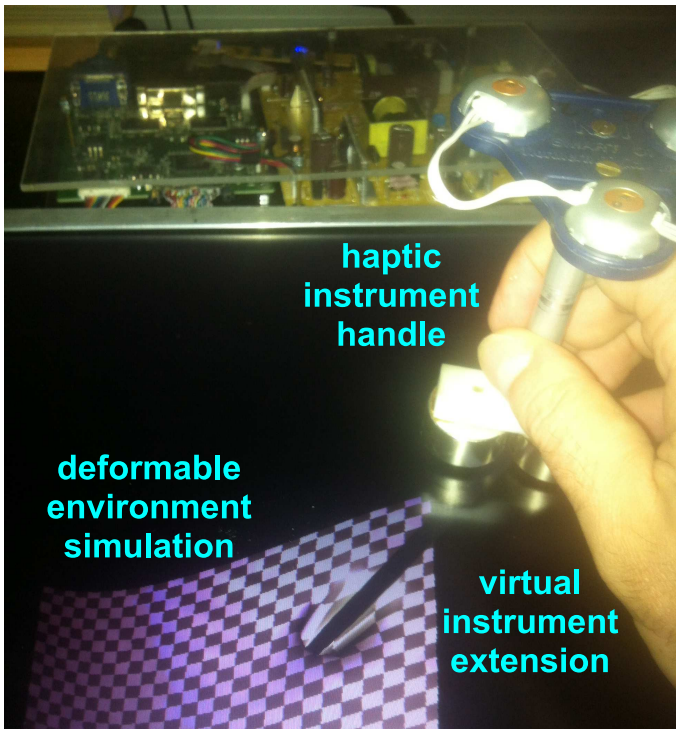

Figure 6: Deformable tissue simulation with grasped tool aligned with graphical scalpel

communication between simulation and magnetic levitation threads with a haptic update rate of 1000 Hz. Alternatively, haptic rendering and dynamic simulation calculations can be performed synchronously with the motion tracking at 860 Hz.

A. Software Implementation

Four basic simulations were written to demonstrate the capabilities of the colocated haptic system. All simulations made use of the 3D-parallax, head tracking, and haptic capabilities of the system. All but one made use of the system's 6-DOF position sensing and haptic output capabilities. In all cases, head tracking, 3D display, and haptics were run at full speed, and physics calculations were performed at the haptic update rate.

The simplest simulation consists of a ball hanging on a virtual spring whose other end is moved freely by the user. By moving the maglev handle, the user may swing the ball, experiencing inertial forces as well as seeing 3D parallax effects. No torques are experienced by the user.

A second simulation consists of a paddle manipulated by the user in both translation and orientation, and a ball that the user may bounce on the paddle. This demonstration presents the user with stronger and more variable haptic feedback, this time including gentle torques based upon the location of the paddle-ball contact.

The third simulation consists of a rectangular user-controlled peg and a rectangular hole into which the user may insert the peg. Edge-edge, edge-face, and vertex-face contacts are all posible and result in both forces and torques applied to the haptic instrument handle. While inserted into the hole, haptic feedback is sufficiently stable that the user may safely let go of the instrument handle, leaving the virtual hole walls to support the handle. This demonstration involves stiff haptic feedback in both forces and torques.

The final and most sophisticated simulation consists of a virtual tool controlled by the user and a deformable surface with which the user may interact. The deformable surface is modeled by a hexahedral mass-spring-damper lattice. Deformation and jello-like vibration may be observed by the user on contact with the surface.

While the code for display, physics, and haptic feedback differs from program to program, each demo utilizes a common core of simulation software, which provides for head tracking, 3D-rendering, and timing of physics, graphics, and haptics calculations.

The code for the magnetic levitation system controller was collected into a separate software library, modelled on the MLHI library provided by Butterfly Haptics LLC for their haptic device. This library provides for initiating and shutting down the haptic device, conveying feedback forces to it, and for performing PD control of the haptic device position.

B. Multithreading and Timing

Each of the simulations makes use of multithreading to manage the different timing requirements of graphics, head tracking, and physics/haptic feedback, while still providing low-latency feedback. Each of these tasks is allocated a thread. Communication between threads is performed through data structures stored in global memory.

In order to more easily ensure low-latency feedback, this communication is not synchronized. As no more than one thread writes to a given set of data, the data sets are small, and changes to data between frames tend to be small, error due to threading conflicts is imperceptible to the user.

The program begins by initializing data structures, then launching threads for head tracking and physics. The main thread then assumes the role of running graphics. Haptics is initiated later by the user.

The graphics thread is managed by the freeGLUT library, an open source alternative to the OpenGL ulility toolkit. It is responsible for displaying the current state of the simulation data structures, which it does at the display rate of the 3D monitor (120 frames per second). The freeGLUT library uses the same thread to manage keyboard input to the simulation.

Meanwhile, the head tracking thread initializes and repeatedly queries the NDI Polaris for the location of the user's head. If this position can be determined, the translation and orientation of the user's head is calculated and stored in

2013, © Copyright by authors, Published under agreement with IARIA - www.iaria.org

global memory. This happens at the update rate of the Polaris sensor, which is about 10 Hz.

Finally, a third thread runs the simulation. At the beginning of the program, haptics is not initiated, and so this thread just performs physics calculations, running in a loop at approximately the rate of the maglev controller (860 Hz). When haptics is initiated, a transition is made from running in a loop to running in a callback from the device controller code. Once this has happened, the code runs at the rate of the device controller and haptic rendering is performed in addition to the simulation. When haptics is deactivated a transition is made back to running in a loop.

Upon receiving a command to exit the program, each of the threads shuts down in turn. Next, logging data, if any, is stored, then the program exits.

C. Coordinate System Correspondance

In the colocated haptic system, the size of the display and its location relative to the user's eyes is known. As a result, the apparent locations of virtual objects correspond in a one-to-one fashion to real locations: virtual objects may be considered as embedded in real space. For example, a virtual ball may be thought of as being 2 cm in diameter and located 4 cm below the display. Using information about the location of the user and size of the display, that virtual ball may be rendered on the display so that to the user's eye it appears to be 2 cm in diameter, 4 cm below the center of the display, no matter where the user moves.

Accordingly, virtual units and coordinate systems take on more meaning when used with the colocated system. For simplicity, it was chosen to locate the origin of the virtual coordinates at the center of the 3D display, with coordinate axes aligned to the display's edges, with units of mm.

It is interesting to note that due to the correspondence of virtual and real locations, the simulations' virtual coordinate system is also a coordinate system for the real space surrounding the display. Calculating the location of the user's head in real space also calculates the location of the user's head in virtual space.

D. Deformable Surface Modeling and Simulation

The deformable surface simulation was designed to demonstrate the possibility of sophisticated haptic environments involving non-rigid contacts and complicated geometry. The deformable "landscape" consists of an approximately regular mass-spring-damper lattice whose top side varies in height according to a heightmap. The construction of the landscape proceeds in 3 phases: calculation of the height map, distribution of point masses, and finally, linking neighboring point masses by springs.

The height map consists of a rectangular array of heights, in millimeters, indexed by x and y positions. The heights are either calculated in a pseudo-random fashion or according to a simple function, such as a sine wave. This is enough to determine the surface that the user sees.

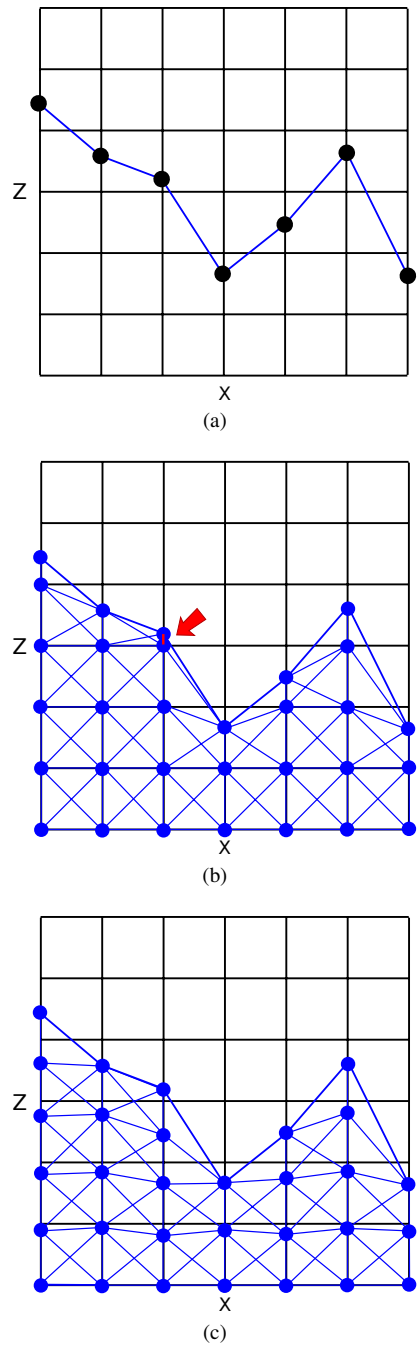

Figure 7: Building the lattice from a heightmap

The next step is to generate the lattice points beneath the heightmap. To do this, a three dimensional grid is placed over the heightmap. Each point of the grid below the corresponding surface point is made into a point mass of the lattice. A slice of the grid and an example heightmap is pictured in Figs. 7a –7c. In order to avoid unusually short

2013, © Copyright by authors, Published under agreement with IARIA - www.iaria.org

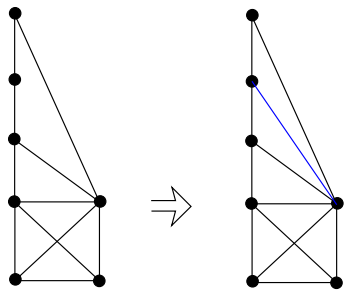

Figure 8: Additional links added when surface vertices are far apart

links (as in Fig. 7b), the masses in each column are respaced uniformly rather than on the points of the grid (Fig. 7c). This means horizontally adjacent vertices in the grid will not be at exactly the same heights in space. All vertices are assigned the same mass, except for the vertices on the bottom and edges, which are assigned infinite mass, to keep them stationary.

The final step is to link the lattice points together. In order to prevent undesirable inversions of the grid, for each grid point, each of the up to 26 horizontal, vertical, and diagonal neighbors of the grid point are linked to it. Adjacent surface vertices that are not already linked together are then linked together. Finally, each of the vertices below a surface vertex but above an adjacent surface vertex are linked to the lower surface vertex. This can be seen in Fig. 8. All of the links are assigned the same stiffness and damping constants.

During physics calculations, a collision detection routine determines the force the user is applying to the point masses. The opposite forces and corresponding torques are added and sent to the haptics device for force feedback. Next, the forces on the point masses due to spring compression and damping are calculated and added to the user's applied force. An Eulerian integration scheme is then used to update the velocity and position of each point mass.

VI. Results

Force and position experimental data in x, y, and z directions obtained during interactive simulations are presented in Figs. 9 and 10. The position data was measured by the position tracking system, and the force data are calculated by the simulations and generated by the coil array of the magnetic levitation system in real time. The commanded forces were shown to be within 0.1 Newtons of force sensor measurements throughout the range of the magnetic levitation system in [19].

The Fig. 9 plots are from a haptic peg-in-hole simulation in which a 25 mm square peg is controlled by the haptic instrument handle and inserted into a 27x54 mm, 10 mm deep square hole. The Fig. 10 plots are from a deformable simulation in which a pointed virtual instrument contacts a deformable object, as shown in Fig. 4. For both cases, haptic

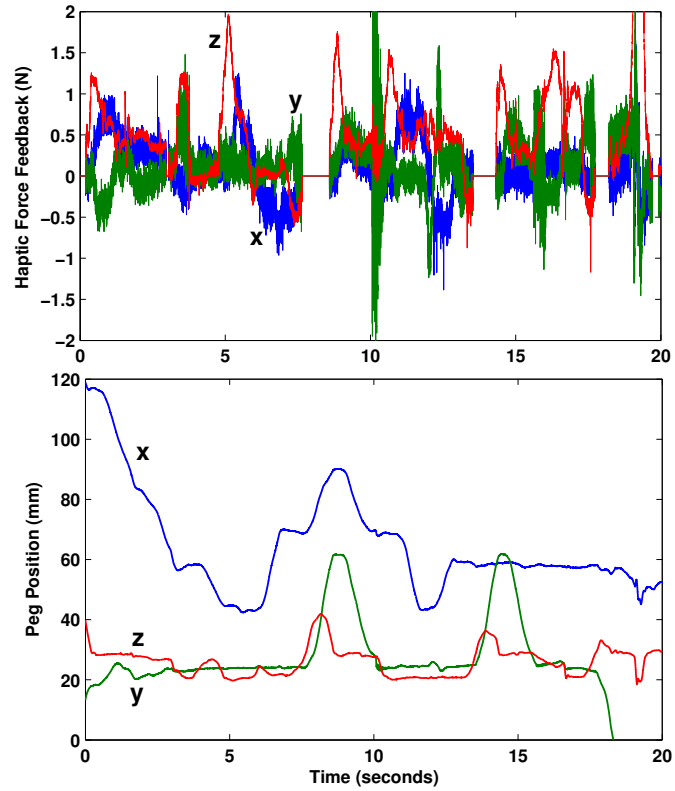

Figure 9: Interactive peg-in-hole simulation data

forces and torques are zero while the instrument is moving freely, contact forces are approximately proportional to the depth of contact, and haptic torques depend on each contact force and the displacement between the contact point and the center of the haptic instrument and simulated tool.

In the peg-in-hole simulation of Fig. 9, the peg is not in contact with the hole or top surfaces at the 8-9 and 14-15 second intervals, the z coordinate is greater than 30, and there is no haptic force feedback. As the peg is moved in and out of the hole, the z position moves between 20 and 30 mm. The x position can vary between approximately 40 and 70 mm while the peg is in the hole, as the hole is more than twice as wide as the peg in the x direction. Non-zero x and y forces are present when the virtual peg is pushed against any of the four sides of the virtual hole. Contact stiffnesses are approximately 0.4 N/mm and the kinetic and static friction coefficents are 0.15 in the simulations.

For the deformable surface of Fig. 10, the probe is moved across the surface during the 12-20 second interval, and the surface is struck with the probe several times in the interval from 8 to 12 seconds. The object was modeled with millimeter-scale surface variations rather than a smooth flat surface. Therefore, this surface texture produces variable vertical (z) forces in response to horizontal (x and y) motions of the intstrument tip. Oscillations in both the position

2013, © Copyright by authors, Published under agreement with IARIA - www.iaria.org

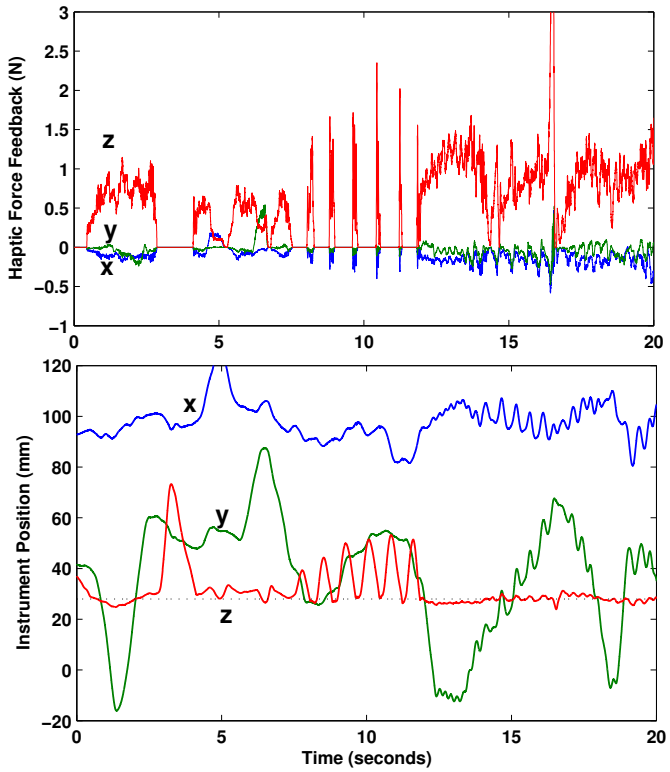

Figure 10: Interactive palpation of deformable surface data

and force data can be seen in the 12-20 second period due to sticking and slipping of the sliding surface contact. Overall the force plots are smoother in the deformable surface simulation than the peg-in-hole simulation due to the compliance and lower friction of the deformable surface.

VII. Future Work

At present, the magnetic levitation and motion tracking aspects of our system are fully developed, but the interactive environments are at a preliminary stage. We plan to refine the detail and physical realism of the simulated environments to a degree where they are useable and can provide measureable benefits in medical training tasks such as surgery, intubation, and needle driving. User studies will be conducted to evaluate the benefits of colocated haptic and graphical training of simulated medical procedures.

The complexity of the modelled environment and the sophistication of the simulated dynamics can be improved by using the graphics processor for additional numerical computations, as a general purpose graphics processing unit or GPGPU. NVIDIA provides the CUDA [37] programming interface to utilize the parallel processing capabilities of the GPGPU on the graphics cards used, however, the physical simulation programming must be completely reformulated to realize these benefits.

One more planned improvement to be made on the system is to reconfigure the system to be simpler and more compact. The optical localizer presently in use is over 1.1 m in length and 18 kg and must be fixed at least 1.5 m from the sensed position markers, which necessitates the use of a large rigid frame assembled from aluminum extrusions. Compact localizer systems such as the AccuTrack from Atracsys have specifications with comparable accuracy, update rates, and latency as needed for stable levitation and haptic feedback, yet are much smaller and can be mounted as close as 0.15 m to the position markers on the handheld instrument. It may also be possible to use electromagnetic sensing systems to track the magnet locations [38], however, interference from the actuator coil currents may need to be overcome to realize sufficient positioning accuracy.

VIII. Conclusion

Our system is the first to combine high-fidelity haptic interaction through a magnetic levitation coil array with interactive virtual environments displayed in 3D in a co-located manner, where the handheld tool grasped by the user is manipulated in the same tabletop space as the perceived 3D graphics display of the simulated environment. The motion range of the magnetic levitation haptic interface device in both translation and rotation is well suited to human hand motions and tabletop displays.

The operation of the system was demonstrated with 6-DOF haptic interactive simulations with solid objects incorporating rigid-body dynamics and deformable surfaces. Continual increases in the the computational speed and capacities available from standard PC hardware, combined with the increasing availability of sophisticated graphics, modeling, and physical simulation programming interfaces, lead to the feasibility of sophisticated interactive medical simulations which could be used with theis co-located haptic and graphic interface system.

Our co-located haptic and graphic interface system is novel in that there is no hardware between the user and the display other than the handheld interaction instrument. The 3D environment is displayed close to the surface of the monitor, so there is no conflict between visual convergence and focal ranges. Electromagnetic force and torque actuation is used for haptic interaction rather than a motorized linkage, providing advantages in backdriveability, precision, and response frequency bandwidths.

We have demonstrated the feasibility and function of our system with the basic simulation environments described.

Acknowledgment

This work was supported in part by National Science Foundation grants IIS-0846172 and CNS-0551515, and by the University of Hawaii College of Engineering.

2013, © Copyright by authors, Published under agreement with IARIA - www.iaria.org

REFERENCES

[1] P. Berkelman, S. Bozlee, and M. Miyasaka, "Interactive dynamic simulations with co-located maglev haptic and 3D graphic display," in *International Conference on Advances in Computer-Human Interactions*, February 2013, pp. 324–329.

[2] C. Luciano, P. Bannerjee, L. Florea, and G. Dawe, "Design of the ImmersiveTouch: a high-performance haptic augmented virtual reality system," in *11th International Conference on Human-Computer Interaction*, Las Vegas, August 2005.

[3] Y. Yokokoji, R. Hollis, and T. Kanade, "WYSIWYF display: A visual/haptic interface to virtual environment," *Presence*, vol. 8, no. 4, pp. 412–434, August 1999.

[4] P. Olsson, F. Nysjo, S. Siepel, and I. Carlbom, "Physically co-located haptic interaction with 3d displays," in *IEEE Haptics Symposium*, Vancouver, March 2012, pp. 267–272.

[5] C. Swindells, M. Enriquez, K. MacLeand, and K. Booth, "Co-locating haptic and graphic feedback in manual controls," Computer Science, University of British Columbia, Tech. Rep. TR-2005-28, 2005.

[6] L. Lin, Y. Wang, Y. Liu, and M. Sato, "Application of pen-based planar haptic interface in physics education," in *International Conference on Computer-Aided Design and Computer Graphics*, September 2011, pp. 375–378.

[7] H. Noma, S. Yoshida, Y. Yanagida, and N. Tetsutani, "The proactive desk: A new haptic display system for a digital desk using a 2-DOF linear induction motor," *Presence: Teleoperators and Virtual Environments*, vol. 13, no. 2, pp. 146–163, April 2004.

[8] D. Swapp, V. Pawar, and C. Loscos, "Interaction with haptic feedback and co-location in virtual reality," *Presence*, vol. 10, no. 1, pp. 24–30, April 2006.

[9] G. Jansson and M. Ostrom, "The effects of co-location of visual and haptic space on judgements of form," in *Euro-Haptics*, Munich, June 2004, pp. 516–519.

[10] R. L. Hollis and S. E. Salcudean, "Lorentz levitation technology: a new approach to fine motion robotics, teleoperation, haptic interfaces, and vibration isolation," in *Proc. 6th Int'l Symposium on Robotics Research*, Hidden Valley, PA, October 1993.

[11] S. Salcudean and T. Vlaar, "On the emulation of stiff walls and static friction with a magnetically levitated input-output device," in *ASME IMECE*, Chicago, November 1994, pp. 303–309.

[12] P. J. Berkelman, R. L. Hollis, and S. E. Salcudean, "Interacting with virtual environments using a magnetic levitation haptic interface," in *Int'l Conf. on Intelligent Robots and Systems*, Pittsburgh, August 1995.

[13] P. J. Berkelman and R. L. Hollis, "Lorentz magnetic levitation for haptic interaction: Device design, function, and integration with simulated environments," *International Journal of Robotics Research*, vol. 9, no. 7, pp. 644–667, 2000.

[14] P. Berkelman and M. Dzadovsky, "Extending the motion ranges of magnetic levitation for haptic interaction," in *Eurohaptics Conference and Symposium on Haptic Interfaces for Virtual Environment and Teleoperator Systems*, Salt Lake City, March 2009, pp. 517–522.

[15] T. Massie and K. Salisbury, "The PHANToM haptic interface: A device for probing virtual objects," in *Proceedings of the ASME Winter Annual Meeting, Symposium on Haptic Interfaces for Virtual Environment and Teleoperator Systems*, Chicago, Illinois, November 1994.

[16] *Novint Falcon User Manual*, Novint Technologies Inc., 2007.

[17] S. Grange, F. Conti, P. Rouiller, P. Helmer, and C. Baur, "Overview of the delta haptic device," in *Eurohaptics*, Birmingham, July 2001, pp. 164–166.

[18] P. Berkelman, "A novel coil configuration to extend the motion range of lorentz force magnetic levitation devices for haptic interaction," in *IEEE/RSJ International Conference on Intelligent Robots and Systems*, San Diego, October 2007.

[19] P. Berkelman and M. Dzadovsky, "Magnetic levitation over large translation and rotation ranges in all directions," *IEEE/ASME Transactions on Mechatronics*, vol. 18, no. 1, pp. 44–52, 2013.

[20] N. J. Groom and C. P. Britcher, "A description of a laboratory model magnetic suspension testfixture with large angular capability," in *IEEE Conference on Control Applications*, Dayton, September 1992, pp. 454–459.

[21] M. B. Khamesee and E. Shameli, "Regulation technique for a large gap magnetic field for 3d non-contact manipulation," *Mechatronics*, vol. 15, pp. 1073–1087, 2005.

[22] D. Baraff, "Interactive simulation of solid rigid bodies," *IEEE Computer Graphics and Applications*, vol. 15, pp. 63–75, 1995.

[23] D. Baraff and A. Witkin, "Dynamic simulation of non-penetrating flexible bodies," in *Computer Graphics* (*Proc. SIGGRAPH*), vol. 26. ACM, July 1992, pp. 303–308.

[24] J. Allard, S. Cotin, F. Faure, P.-J. Bensoussan, F. Poyer, C. Duriez, H. Delingette, and L. Grisoni, "Sofa an open source framework for medical simulation," in *Medicine Meets Virtual Reality (MMVR'15)*, Long Beach, USA, February 2007.

[25] M. Marchal, J. Allard, C. Duriez, and S. Cotin, "Towards a framework for assessing deformable models in medical simulation," in *International Symposium on Computational Models for Biomedical Simulation*, London, July 2008.

[26] J. Barbic and D. James, "Six-dof haptic rendering of contact between geometrically complex reduced deformable models," *IEEE Transactions on Haptics, preprint published online*, June 2008.

[27] D. James and D. Pai, "A unified treatment of elastostatic and rigid contact simulation for real time haptics," *Haptics-e*, vol. 2, no. 1, 2001.

2013, © Copyright by authors, Published under agreement with IARIA - www.iaria.org

[28] C. Zilles and J. Salisbury, "A constraint-based god-object method for haptic display," in *Int'l Conf. on Intelligent Robots and Systems*, Pittsburgh, August 1995.

[29] J. Colgate, M. Stanley, and J. Brown, "Issues in the haptic display of tool use," in *Int'l Conf. on Intelligent Robots and Systems*, Pittsburgh, August 1995.

[30] *HAPI Manual*, 1st ed., SenseGraphics Inc., May 2009.

[31] F. Conti, D. Morris, F. Barbagli, and C. Sewell. *CHAI 3D*. Online: http://www.chai3d.org, 2006.

[32] *Magnetic Levitation Haptic Interface API Reference Manual*, 1st ed., Microdynamic Systems Lab, Carnegie Mellon University, September 2008.

[33] P. Berkelman, M. Miyasaka, and J. Anderson, "Co-located 3d graphic and haptic display using electromagnetic levitation," in *IEEE Haptics Symposium*, Vancouver, March 2012, pp. 77–81.

[34] P. Berkelman and M. Dzadovsky, "Novel design, characterization, and control method for large motion range magnetic levitation," *IEEE Magnetics Letters*, vol. 1, January 2010.

[35] S. Wolfram, *The Mathematica Book*, 5th ed. Wolfram Media, 2003.

[36] O. Chubar, P. Elleaume, and J. Chavanne, "A three-dimensional magnetostatics computer code for insertion devices," *Journal of Synchrotron Radiation*, vol. 5, pp. 481–484, 1998.

[37] *Nvidia CUDA Compute Unified Device Architecture Programming Guide 1.0*, Nvidia, 2007.

[38] C. Hu, M. Li, W. Yang, R. Zhang, and M.-H. Meng, "A cubic 3-axis magnetic sensor array for wirelessly tracking magnet position and orientation," *IEEE Sensors Journal*, vol. 10, no. 5, pp. 903–913, 2010.

2013, © Copyright by authors, Published under agreement with IARIA - www.iaria.org